



UNIVERSITY OF LEEDS

This is a repository copy of *Timing of uplift and evolution of the Lüliang Mountains, North China Craton*.

White Rose Research Online URL for this paper:
<http://eprints.whiterose.ac.uk/89024/>

Version: Accepted Version

Article:

Zhao, JF, Liu, CY, Mountney, N et al. (4 more authors) (2016) Timing of uplift and evolution of the Lüliang Mountains, North China Craton. *SCIENCE CHINA Earth Sciences*, 59 (1). pp. 58-69. ISSN 1674-7313

<https://doi.org/10.1007/s11430-015-5153-z>

Reuse

Unless indicated otherwise, fulltext items are protected by copyright with all rights reserved. The copyright exception in section 29 of the Copyright, Designs and Patents Act 1988 allows the making of a single copy solely for the purpose of non-commercial research or private study within the limits of fair dealing. The publisher or other rights-holder may allow further reproduction and re-use of this version - refer to the White Rose Research Online record for this item. Where records identify the publisher as the copyright holder, users can verify any specific terms of use on the publisher's website.

Takedown

If you consider content in White Rose Research Online to be in breach of UK law, please notify us by emailing eprints@whiterose.ac.uk including the URL of the record and the reason for the withdrawal request.



eprints@whiterose.ac.uk
<https://eprints.whiterose.ac.uk/>

Uplifting Timing and Evolution Processes of the Lüliang Mountain, in Middle Part of North China Craton

Junfeng Zhao^{1,2}, Chiyang Liu^{1,2}, Nigel.P. Mountney³, Jianjun Lu^{1,2}, Yao Yang^{1,2},
Jianghua Qiao^{1,2}, Jilong Cao^{1,2}, Rui Xue^{1,2}

1. State Key Laboratory of Continental Dynamics, Northwest University, Xi'an, 710069;
2. Department of Geology, Northwest University, Xi'an, 710069
3. School of Earth and Environment, University of Leeds, Leeds, LS2 9JT, UK

ABSTRACT: The significance of the study on uplifting and evolution of the Lüliang Mountain lies in its importance to reconstruct the eastern sedimentary boundary of the Ordos basin, as well as its implication for revealing the evolution and breakup of the North China Craton (NCC). The thoughts to research on reformed basin and basin-mountain coupling are followed in this paper. Based on systematic sampling for fission track analysis, it is suggested that the obvious uplifting activities of the Lüliang Mountain occurred since late Early Cretaceous. Three evolution stages namely slowly uplifting (120Ma- 65Ma), accelerated uplifting (65Ma- 23Ma), and intensive uplifting (23Ma to date) can be identified further, among which the uplifting activity since Cenozoic is the major lifting period. The lifting activity exhibits non-equilibrium in temporal and spatial aspects. The middle and northern parts uplifted earlier than the southern part of Lüliang Mountain area. The intensive uplifting activity especially since Miocene had the genetic coupling relationship with the eastern neighboring Shanxi Cenozoic graben system. The uplifting and evolution processes of the Lüliang Mountain area since late Early Cretaceous share an unified regional geodynamic setting, accompanied with lifting and dying out of the Mesozoic Ordos basin and development of neighboring Cenozoic faulted grabens, are mainly related to the far field effects of both compression sourced from southwestern Tibet Plateau and westward subduction of the Pacific block in Cenozoic.

KEY WORDS: Uplifting; fission track analysis; basin-mountain coupling; the Lüliang mountain; the Ordos basin; North China Craton

1 INTRODUCTION

The Lüliang Mountain is located in the middle part of North China Craton (NCC). It appears as a large-scale uplift approximately along NNE-SSW orientation, stretching about 400km long from north to south and with an altitude ranged from 1500m to 2831m. As one of the major mountains in the NCC, the Lüliang Mountain adjoins the Cenozoic Shanxi Graben to its eastern boundary; neighbors to the Ordos Basin along the Lishi Faults Zone (Fig. 1). The discussions about the original sedimentary boundary of Ordos Basin during Mesozoic are existed for decades. For lack of constraint on the uplifting timing of the Lüliang Mountain, the eastern sedimentary extent of the Ordos Basin is still controversial (Ye et al., 1983; Zhang et al., 1983; Li et al., 1992; Sun et al., 1985; Liu et al., 2008; Cheng et al., 1997; Wang and Zhang, 1999; Zhang

et al., 2008; Zhao et al., 2006; Yang et al., 2012). In addition, the study about the uplifting time and evolution processes of the Lüliang Mountain is a key scientific issue contributed to further clarify the structural framework, tectonic setting and destruction process of the central NCC, as well as helpful to understand the basin attribution of the Mesozoic Ningwu-Jingle, Datong coal-bearing basins in and around the Lüliang Mountain area.

The existed study about the Lüliang Mountains area mainly focused on the geological events about pre-Cambrian, establishment of chronology framework (Shen et al., 1963; Geng et al., 2000; Xu et al., 2008) and the early evolution of the NCC (Zhao et al., 1990; Timothy and Li, 2003; Zhao et al., 2008). The uplifting time and its evolution process began to be concerned in recent years. Based on sedimentology and 4 suites of fission track data analysis, Zhao et al. (2009) initially revealed the possible uplifting timing which is from the end of Mesozoic to early Cenozoic. According to analysis on the distribution and magnetostratigraphy dating of Neogene red clay in the Lüliang Mountain area, Li Jianxing identified an uplifting event episode happened during late Pliocene (Li et al., 2009; Li et al., 2013). Limited by sparse dating samples, previous studies only provided partial information about the Lüliang Mountain. There still is a lack of further detailed evidence about the time, evolution process and spatial-temporal differentiation in the Lüliang Mountain area. Furthermore, the relationship between the Lüliang Mountain and its adjacent Ordos basin during Mesozoic to Cenozoic is still scarce. Some related scientific problems are blocked to further discussion as a result.

Fission-track analysis is an effective method of thermochronology, which based on annealing behavior of spontaneous fission tracks of

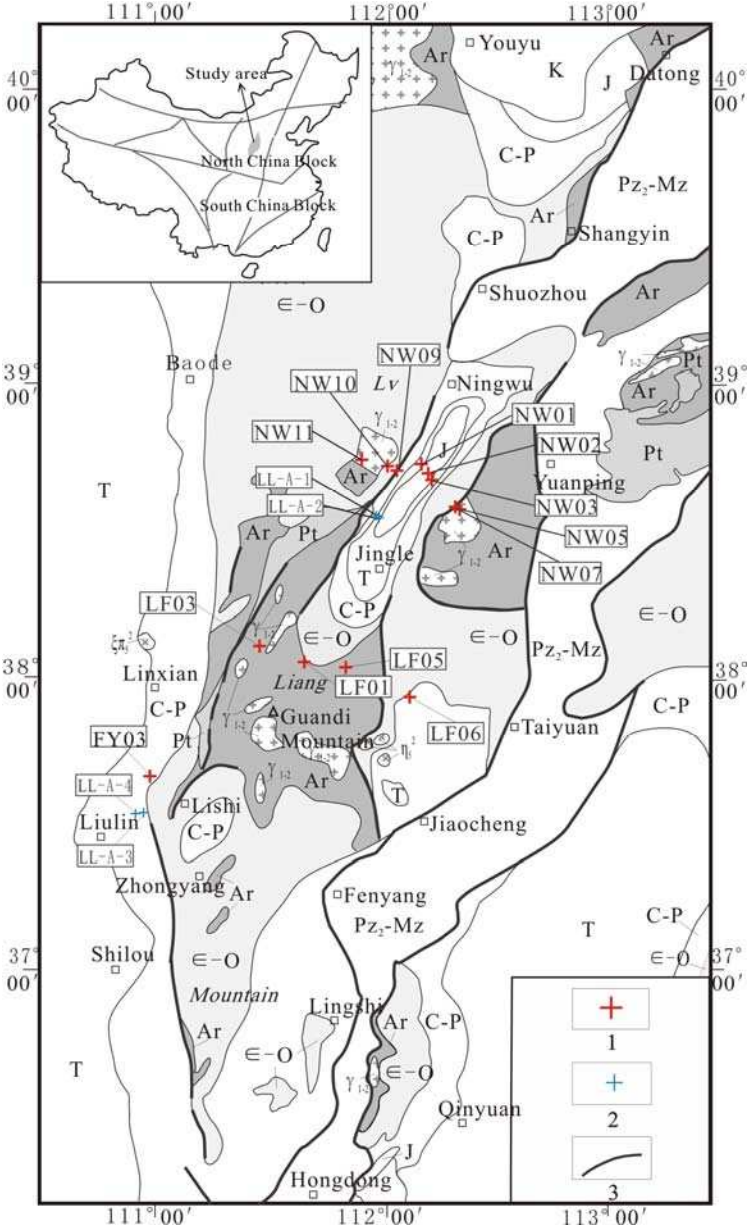


Fig.1 Pre-Cenozoic geological map of the Lüliang Mountain area and samples location

1- samples location in this study; 2- published samples location by the author; 3- main faults

some ^{238}U bearing minerals such as apatite, zircon during geological span, which is widely employed to analyze the multiple periods' uplifting, denudation process and mechanics of various mountains at home and abroad (Peter, 2005; Donelick et al., 2005). Lots of case studies and a series of successful explanations are achieved in the last decades. Honestly, there are some limitations and suit conditions about this method. For instance, if the samples experienced complex thermal history or partial annealing, their thermal history are difficult to recover. For those samples experienced cooling process less than 60°C (above apatite annealing belt), represented late Neogene uplifting event, there is a lack of qualified constraint. Combined the features of fission track analysis method and the actual geological background of studied area, the thought on basin-mountain coupling (Liu et al., 2005; Wang and Li, 2003; Zhang et al., 2006; Liu et al., 2009) are adopted, fission-track thermochronology analysis is specially employed, combined with analysis of stratigraphy and depositional record responses, integrated profiling, the uplifting time and detailed evolution process of the Lüliang Mountain during Mesozoic-Cenozoic are discussed in this paper.

2 GEOLOGICAL BACKGROUND

According to current tectonic deformation appearance, the Lüliang Mountains area can be divided into several sub-structural units, including Lüliang compound anticline, Luya Mountain compound anticline, Ningwu-Jingle compound syncline (Zhao, 1990).

The Ningwu- Jingle area located in the north is a compound syncline structure comprised of the Jurassic, Triassic and Carboniferous-Permian strata. To the central part, Loufan and Fang Mountain area make up of the core of Lüliang compound anticline, exposed metamorphic rocks and intrusive rocks of Archeozoic and Proterozoic. To the south, it exhibits as compound syncline and anticline structures made up of Upper Paleozoic and Lower Paleozoic strata. Previous studies suggest that the Lüliang Mountains area is located at the conjunctive position of the final cratonization between the eastern block and the western block of NCC as a result of their collision and matching from New Archaean era to Middle Proterozoic Era (Timothy and Li, 2003; Zhao et al., 2008). During the early Paleozoic, the Lüliang Mountain area exhibited as an inherited ancient land originally, then suffered erosion and gradually disappeared processes. The conglomerate bed appears at the bottom of Cambrian System in Lishi area, which shows unconformable contact relationship with its underlying Archean gneiss, was the product of erosion from neighboring ancient land and accumulated around the provenance area. The paleo-uplift submerged gradually accompanied with enhanced transgressive process during Middle to Late Cambrian (Wang, 1995). The Lüliang Mountains area along with central part of Shanxi province accepted lagoon or carbonate deposition in Ordovician period. The Ordovician strata mainly comprised of dolomite and limestone rock with a thickness of 500~600m (Feng, 1990).

The Upper Paleozoic is widely developed in and around the Lüliang Mountain area with a thickness of about 1200m. There experienced a sedimentary environment evolution from lagoon, tidal flat, carbonate platform to delta and fluvial system and so on (Shang, 1997; Fu et al., 2003).

As far as the west of NCC in the late Paleozoic, their priority provenance area is sourced from the northern Inner Mongolia-Yin Mountain. There isn't a paleo-uplift structure existed in the Lüliang Mountain area which could provide sedimentary source and separate the NCC

into two parts.

A fluvial- lacustrine clastic dominated succession deposited in the western NCC during Late Triassic-Middle Jurassic. Residual Triassic and Jurassic strata still existed in and around the Lüliang Mountain area, such as the Ninwu-Jingle basin, south west Taiyuan city and Qinshui basin and so on. Furthermore, it exhibits a gradual transitional relationship with the residual Ordos basin in respects of lithofacies and its association (Cheng et al., 1997; Liu et al., 2008; Zhao et al., 2010).

After the late Jurassic tectonic compression and denudation, there accepted a widespread fluvial-aeolian succession in the western NCC in early Cretaceous. Erosion strata thickness restoration suggests that the Lower Cretaceous strata deposition should be extended to the Lüliang Mountain area (Weng et al., 2009). During the late Cretaceous, there have no sedimentary records both in the Lüliang Mountain area and the Ordos basin. Finally, Pliocene red clay layer and Quaternary loess both originated from aeolian transportation widely spread in the Lüliang Mountain area and its neighboring Ordos basin. The Shanxi Grabens located to the east of Lüliang Mountains subsided in succession since Neogene period.

3 SAMPLES AND ANALYSIS METHOD

In order to comprehensively depict the differentiation of uplifting time and evolution process in spatial and temporal aspects, three sampling sections are designed from the north to the south in the Lüliang Mountain area, with 22 suites of samples are selected for fission track analysis. Because of the main sampled rock type in the middle and south sections are Cambrian-Ordovician limestone and dolomite, which are lack of enough apatite grains. 10 suites of samples are failed to achieve enough mineral grains. As a result, we obtained 12 suites of AFT data in north and middle sampling sections totally as well as 4 suites of ZFT data in middle sampling section.

The collected rock samples were crushed and abraded after primary separation, the apatite and zircon were concentrated using heavy liquid and magnetic separation. Apatite grains using epoxy resin ground and polished to an optical finish to expose the internal grain surface. The analysis of fission track adopted the external detector method. Spontaneous tracks were etched to exposing by 7% HNO₃ for 30s at 25°C. Muscovite was used as an external detector which was etched after irradiation in 40% HF for 20s at 25°C. Neutron fluency was monitored using CN5 uranium dosimeter glass. Fission track was measured using high accuracy optical microscope. Fission track densities in both natural and induced fission track populations were measured and only those crystals with prismatic sections parallel to the c-crystallographic axis were accepted for analysis as these crystals have high etching efficiency. Lengths of horizontally confined fission tracks were measured using the routine which proposed by Green (Gleadow et al., 1986; Green, 1986). Age values were calculated using the IUGS-recommended constant and the equation of calibration fission track approach (Hurford and Green, 1982). The analysis of the samples was completed in Institute of High Energy Physics, Chinese Academy of Sciences. The results of test list in Table 1.

4 EXPERIMENTAL RESULTS

4.1 The Experimental Results of Apatite Fission Track (AFT)

The achieved 12 suites of AFT data show younger apparent ages relative to their hosting

Table 1 The fission track analysis results of apatite and zircon samples in the Lüliang mountain area

Sampling Section	Sample No.	Latitude N	Longitude E	Elevation (m)	Hosted Rock type	Mineral	Times	Number of grains(n)	ρ_s ($10^5/cm^2$) (Ns)	ρ_i ($10^5/cm^2$) (Ni)	ρ_d ($10^5/cm^2$) (N)	P(χ^2) (%)	Central age (Ma) ($\pm 1\sigma$)	Pooled Age (Ma) ($\pm 1\sigma$)	L(μ m) (N)	
North	NW01	38° 51' 18.20"	112° 11 '2.5"	1759	Sandstone	Apatite	T	29	1.904 (669)	9.886 (3474)	20.841 (9117)	24.1	70 ± 5	71 ± 5	12.6 \pm 2.0 (66)	
	NW02	38°45' 24.77"	112°12'20.51"	1575	Sandstone	Apatite	J2t	28	3.757 (733)	17.978 (3508)	20.575 (9117)	96.0	75 ± 5	75 ± 5	12.8 \pm 2.0 (81)	
	NW03	38°43'55.41"	112°15' 26.59"	1610	Sandstone	Apatite	J2t	28	2.286 (1039)	11.636 (5289)	20.308 (9117)	0.7	70 ± 5	70 ± 4	12.7 \pm 2.5 (75)	
						Zircon	J2t	24	93.027 (4490)	89.982 (4343)	28.264 (13124)	0	130 ± 11	124 ± 6		
	NW05	38°40' 29.85"	112°20' 30.72"	1725	Granite	Apatite	PP	28	1.826 (518)	6.881 (1952)	20.13 (9117)	28.5	94 ± 7	94 ± 7	13.2 \pm 1.8 (92)	
	NW07	38°40' 28.80"	112°21' 13.7"	1745	Granite	Apatite	PP	28	4.139 (789)	12.817 (2443)	19.774 (9117)	29.4	111 ± 8	112 ± 7	12.9 \pm 2.0 (103)	
	NW09	38° 51' 34.20"	112°04' 46.22"	1713	Monzonite	Apatite	PP	28	1.283 (406)	8.985 (2844)	19.596 (9117)	88.0	49 ± 4	49 ± 4	13.1 \pm 2.1 (101)	
	NW10	38° 54' 8.70"	111°55' 23.31"	2108	Mudstone	Apatite	∞ -O	12	12.816 (1576)	35.406 (4354)	19.418 (9117)	0.1	126 ± 9	123 ± 7	12.6 \pm 2.0 (79)	
	NW11	38° 53' 34.46"	111°53' 18.86"	1554	Monzonite	Apatite	PP	24	10.446 (4778)	28.645 (13102)	19.241 (9117)	0	120 ± 8	123 ± 7	12.9 \pm 1.8 (124)	
	Middle	LF01	38° 01' 15.68"	111°40' 18.37"	1300	Diabase	Apatite	MP	28	1.745 (117)	4.818 (323)	18.974 (9117)	100.0	120 ± 14	120 ± 14	12.3 \pm 2.0 (11)
		LF03	38° 0' 38.16"	111°21' 43.2"	1323	Granite	Apatite	PP	28	7.268 (1116)	21.251 (3263)	18.707 (9117)	8.3	111 ± 7	112 ± 7	12.8 \pm 2.1 (104)
LF05		37° 56' 43.62"	111°47' 0.03"	1629	Diabase	Apatite	PP	28	4.65 (895)	13.716 (2640)	18.529 (9117)	63.0	110 ± 7	110 ± 7	13.4 \pm 1.7 (80)	
LF06		37° 57' 12.51"	112°04' 15.62"	1042	Sandstone	Apatite	P	28	1.653 (1091)	12.516 (8259)	18.351 (9117)	28.1	42 ± 3	43 ± 3	13.5 \pm 2.0 (101)	
	Zircon					P	25	105.924 (4217)	68.523 (2728)	28.103 (13124)	0	184 ± 15	183 ± 10			
South	FY03	37° 31' 05.00	111°06' 45.00"	930	Sandstone	Zircon	P	24	89.453 (5188)	82.59 (4790)	27.889 (13124)	86.3	128 ± 7	128 ± 7		

Notes: ρ_s , ρ_i , and ρ_d are spontaneous track density, induced track density (track number over area), and standard track density respectively; N_s , N_i , and N_d are numbers of spontaneous track, induced track, and standard track respectively; L is mean track length ($\pm\sigma$); P(χ^2) is χ^2 test value.

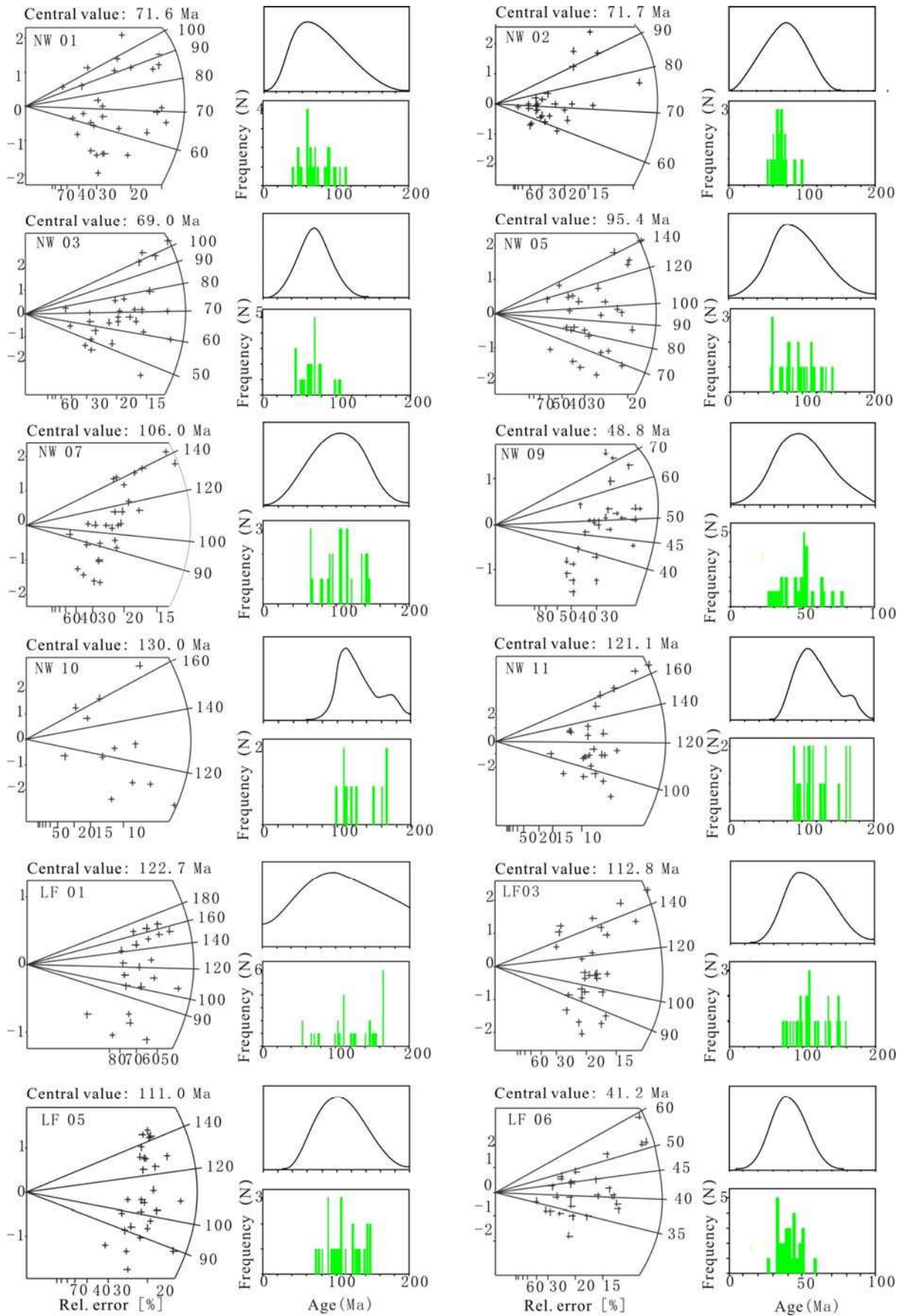


Figure 2 Radial plot, histogram and their frequency curves of single apatite grain ages, 12 samples in total. Legend are given at the last row of the figure.

strata or rock mass forming time. It demonstrated that the samples have experienced completely annealing and could be used to analyze their uplifting process (Tab. 1, Fig. 2). There are 8 suites of data obtained in the north sampling section, among it 6 suites of data have χ^2 values more than 5%. Single-grain age histograms present typical single-peak distributions. The distributive histograms of the track length mainly were single-peak too, which indicates the feature of controlling by single thermal event and shows definite geological thermal meaning. The remaining 2 samples have χ^2 values less than 5%, single-grain ages histograms show double peaks (NW-10) or multimodal (NW-11), and the distribution of fission track length show single-peak. All these features demonstrated that they experienced relative complex thermal history process. The mean track lengths for all the 8 samples range from $12.6\pm 2.0\mu\text{m}$ to $13.20\pm 1.8\mu\text{m}$ and it indicated the samples experienced nearly unanimous thermal evolution background (Fig. 3). The Gauss fitting method is employed to decompose the mixed fission track age of samples NW-10 and NW-11. As a result the younger ages namely 115Ma and 108 Ma are obtained individually to analyze the uplifting history.

There χ^2 values of the 4 samples selected from the middle section were $>5\%$. Single-grain age histograms show wider (LF01, LF03 and LF05) or narrower (LF06) single-peak distribution, which indicates single thermal history evolution. The distribution of fission track lengths of the LF03, LF05 and LF06 were single-peak. While the track length distribution of LF01 was bimodal, possible related to limited number of confined fission track in this sample. The mean track lengths for the 4 samples range from $12.3\pm 2.0\mu\text{m}$ to $13.50\pm 2.0\mu\text{m}$ (Fig. 3).

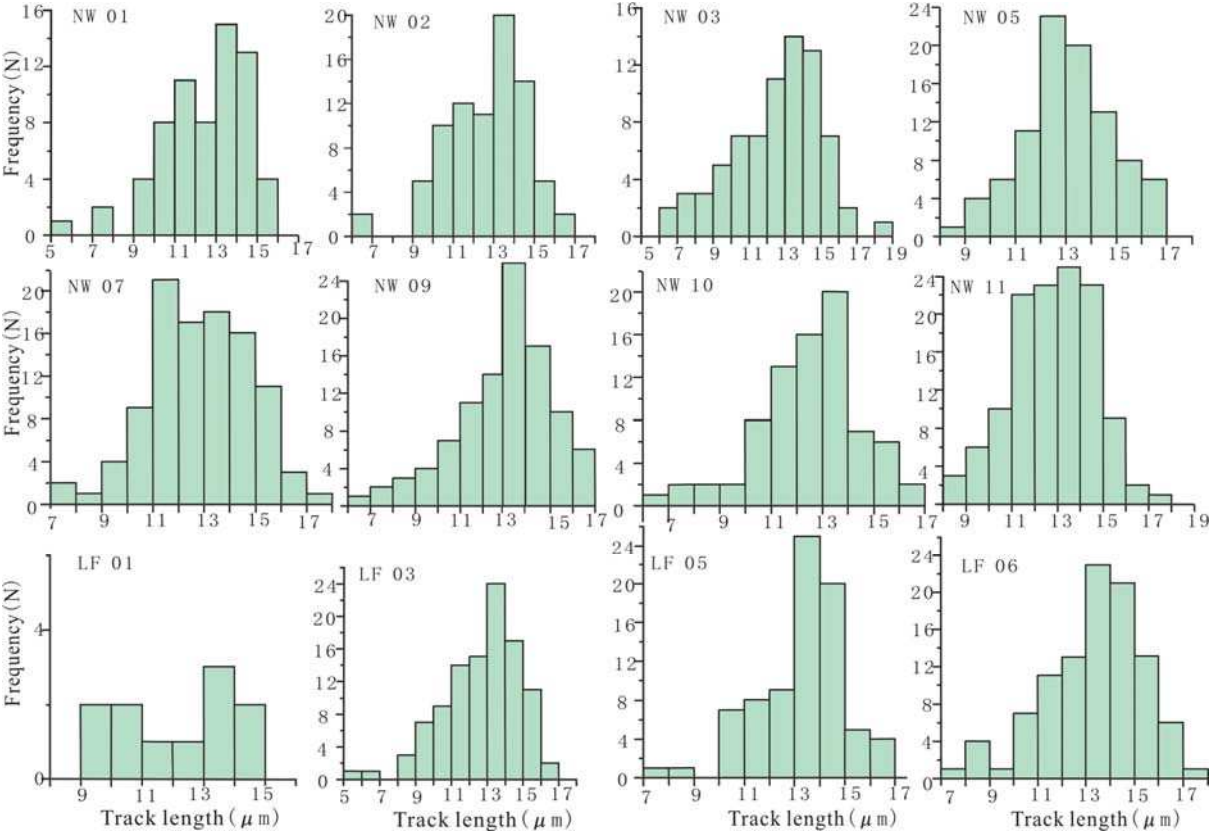


Figure 3 Histograms of the fission track length distribution

4.2 The Experimental Results of Zircon Fission Track (ZFT)

Three suites of ZFT data are achieved in this study. The NW03 sampled from the north section and LF06 sampled from the middle section hosted in the Middle Jurassic Tianchihe Fm. and Upper Paleozoic Shanxi Fm. individually. Their χ^2 values were <5%, single-grain age histograms was single-peak, the elder group of age data were exceed their hosted rock age, which demonstrated these samples experienced incomplete annealing process. Based on the Gauss fitting decomposing, younger age data namely 110Ma and 148 Ma are obtained from the samples NW03 and LF06 individually. The FY03 from south sampling section hosted in Permian feldspar quartz sandstone has a χ^2 value of 86.3%, with a single peak distribution in single-grain age histogram. The central age of FY03 is 128 ± 7 Ma, which is far younger than its hosted strata, and demonstrated entirely annealing process.

5 THE RECONSTRUCTION OF THE UPLIFTING HISTORY

5.1 The Implication for Uplifting Timing and Processes Recorded by AFT

The histogram of the apatite fission track age (including 2 data published by the author previously (Zhao et al., 2009)) shows, fourteen AFT age data in the study area centered into three distinct periods: Early Cretaceous-Late Cretaceous, Late Cretaceous-Paleogene and Early Eocene, which reflecting feature of multiple phases' uplifting process (Fig. 4). All age data sampled along the northern section (NW01, NW02, NW03 and NW09) located in the central part of the Ningwu- Jingle syncline is younger than the data come from either synclinal flank (NW5, NW10 and NW11), indicating that synclinal flank uplifted prior to the core part. The 4 age data at the middle sampled section show a trend of increasing to the compound anticline core, indicating the earliest uplifting happened in the center part of the compound anticline. According to the theory of fission track annealing, if it was an uniform uplift as a whole,

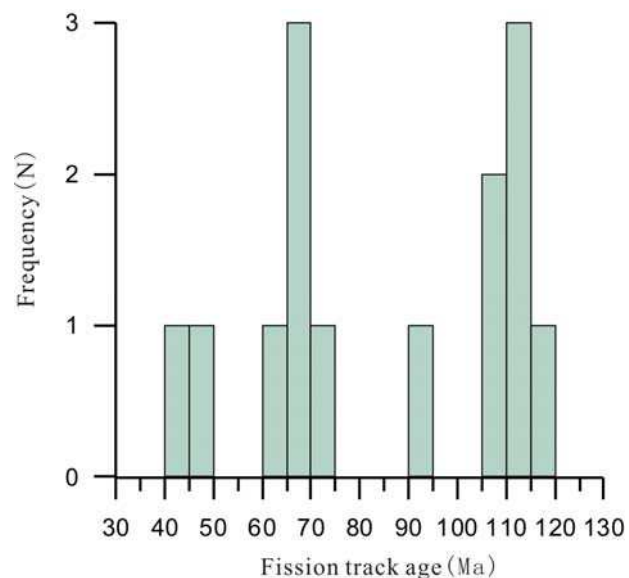


Figure 4 Histograms of the apatites fission track ages distribution for all samples

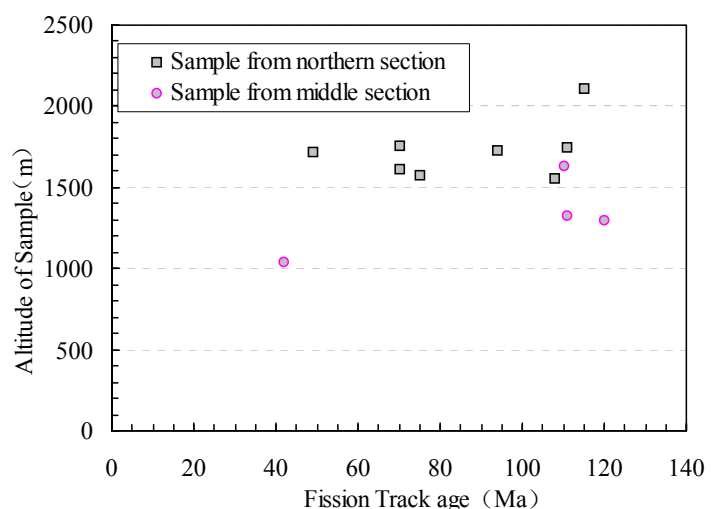


Figure 5 Diagram of the elevation- fission rack age from the Lüliang Mountain

the higher elevation, the smaller fission track age. From the Fig. 5, we can see that the fission track age for samples from different host rocks in the study area is negatively corrected with sample elevation, which illustrates that the relationship of strata superposition has been changed before uplifting and cooling, that is, the fold deformation of strata has occurred before large-scale uplifting. Based on the samples collected from Precambrian basement, the early fold processes with compressive settings occurred between the Early Cretaceous and the Late Cretaceous.

Apatite fission track age records the geologic time of when the host rocks for samples escaped partial annealing zone. Seven data sampled from northern and middle sections in the study area record a widespread compression and uplifting event happened during Early Cretaceous to Late Cretaceous. the uplift processes got the Proterozoic basement lifted upon the partial annealing zone. Based on the ancient geothermal gradient of $30^{\circ}\text{C}/\text{km}$, the ancient surface temperature of $20^{\circ}\text{C}/\text{km}$, Proterozoic rocks were buried to $\geq 2000\text{m}$ before the uplift in Early Cretaceous. The overlying sedimentary covers are Paleozoic-Mesozoic sedimentary strata. Three data sampled in northern section located in Ningwu- Jingle syncline record the uplifting event during the Late cretaceous-Early Paleogene. In other words, the Jurassic strata in Ningwu- Jingle syncline was still at the depth of 2000m or so in Early Paleogene. So it's assumed that there should have been thicker lower Cretaceous deposits overlying the Jurassic strata. The age data of the sample NW09 collected from the west flank of Ningwu- Jingle syncline is 49Ma, younger than adjacent data. It may attribute to its location in the transition parts of the syncline and the compound anticline where the thrust faults developed, possibly records the time of fault activity. The Permian strata hosted sample LF06 located in West hill to Taiyuan city, with the fission track age of 45Ma, indicating an early uplift processes of the eastern flank of Lüliang compound anticline.

Previous studies revealed that Early Cretaceous sedimentary extent of the Ordos basin shrinking westward compared with Triassic-Jurassic periods. Study based on strata thickness recovery suggests that the eastern margin of the original sedimentary boundary could be to the east of present Yellow River (Weng et al, 2009). Due to the analysis on the fission track age of Ningwu-Jingle syncline and Lüliang compound anticline, it can be deduced that in the Early Cretaceous (about 145~120Ma), it was still receiving deposits in the Lüliang mountains area, but since the late Early Cretaceous, due to the regional compression in the central and northern Lüliang mountains area, the strata experienced deformation, resulting in the uplifted regions being the earliest to lift out of the partial annealing zone. Since the Late Cretaceous, the overall uplift of the Ordos basin, Lüliang mountain area also lasted uplifting, resulting in the center of the compound anticline suffering a strong uplifting and denudation , while the center of the Northern syncline uplifted slowly, so it suffered less damage. Until 70-60Ma, the central strata in Ningwu-Jingle syncline uplifted out of the partial annealing zone, the Lower Cretaceous strata was the earliest to suffer from denudation.

The characteristics of the cooling history for samples can also be indicated by the apatite fission track length distribution. Shorter track peaks in the histogram formed inside of the partial annealing zone or near it, while longer track peaks formed after the cooling event. The fission-track length distributions in the study area are generally unimodal, suggesting an obvious controlling by uplifting and cooling processes. At the same time, the track length distributions for samples from the center of Ningwu-Jingle syncline show a trend of gentle to

left side, and steeper to right side, as well as more shorter tracks (Fig. 3). It suggests that these samples have experienced a relatively long-term lingering in the partial annealing zone.

Previous studies shows that widespread uplifting processes occurred since $23\pm 3\text{Ma}$ (Zhao et al, 2009; Li et al., 2013), but we haven't obtain the age data in this study. It is likely that the samples recording the time in the middle and north sections haven't exhumed to the surface. Widespread extensional rifting has occurred around the Ordos basin since Paleogene. Weihe basin was the earliest to experience rifting and subsiding since Eocene. The Sangganhe basin and the Yuncheng basin located to the north and south of Shanxi graben individually began to subside during Oligocene and Miocene respectively. In the adjacent Lüliang mountain, there are AFT age data recording the correlative uplifting event near the graben (Liu et al., 2008; Li et al., 2013). The uplift of the Lüliang mountain and the subsidence of the neighboring grabens in the same period more likely related to tectonic transition of Tibetan Plateau during the Late Oligocene-Early Miocene ($20\pm 2\sim 4\text{Ma}$) as well as the far field effect of the activity around west Pacific tectonic domain (Liu et al, 2009).

5.2 The Geological Information Recorded by ZFT

Three fission track age data of zircon derived from northern, central and southern sections are 110Ma, 148Ma and $128\pm 7\text{Ma}$ respectively. These ages are consistent with the early regional compression and uplift event that the apatite fission track age revealed, also there is possible superposition of Late Jurassic-Early Cretaceous regional thermo-tectonic event (Sun et al., 1997; Ren et al., 2006).

5.3 Thermal History Modeling

Using computer technology to simulate the thermal history, and then revealing the continuous burial and uplift process of samples, is a crucial means of fission track thermochronology in recent years (Yuan et al., 2011; Ketcham, 2005). In this paper, we employed Ketcham et al.'s annealing model (Ketcham, 2005), as well as Monte Carlo method. The initial conditions of modeling are determined by the factors that related to the fission track method and the basic geological characteristics. The constraints of the modeling temperature are from the bottom temperatures (120°C) of fission track annealing zone to the present surface temperatures (20°C). The time of the model is from the early Cretaceous to the present. (Fig. 6) The bold line in each plot represents the best-fit thermal history model, the dark grey regions delineate the good-fit thermal history models, and the light grey regions mark the statistically acceptable models. The factors of Kolmogorov-Smirnov test (K-S test) which compared the measurement between actual fission track length to the modeling are between 0.75~0.93, and the goodness-of-fit (GOF) factors are between 0.74~0.98, which all represent a good fit.

The measured fission track ages from samples NW10 and NW11 along the northern section and samples LF01, LF03 and LF05 along middle section range from 108Ma to 120Ma, which show a consistent cooling path, thus the uplifting process could be divided into three stages. The first stage occurred between 120Ma and 70Ma, during which the Lüliang Mountain was in a slow uplifting process, and the cooling rate was $0.13^\circ\text{C}/\text{Ma}$ to $0.29^\circ\text{C}/\text{Ma}$. The second stage involved a rapid uplifting process from 70Ma to 20Ma, and the cooling rate was about $0.70^\circ\text{C}/\text{Ma}$. The last stage occurred from 20Ma until now, and involved a strong uplifting process during which the cooling rate was $0.75^\circ\text{C}/\text{Ma}$. The three fission track ages of measured samples (70Ma~75Ma) from Ningwu-Jingle syncline in northern section (NW01,

NW02 and NW03) showed a more consistent cooling path, which could also be divided into three stages, the slow uplifting (100Ma~65Ma), the accelerated up lifting (65Ma~12Ma), and the intensive uplifting (12Ma until now).

As we mentioned earlier, about 23 ± 3 Ma, there was a widespread uplifting event in larger region including the southern part of Lüliang Mountain and the eastern Ordos Basin (Zhao et al., 2009; Li et al., 2013), which was accompanied by the subsidence of Cenozoic Shanxi grabens. Especially the Taiyuan Basin and Linfen Basin, located to the east of Lüliang Mountain, which began to rift subsidence and accept deposits until the Pliocene. The Cenozoic strata in Taiyuan Basin show a trend of thicker in the east and thinner in the west, and the thickest strata developed in the western piedmont, ranged from 1000m to 3800 m, show distinct controlling by piedmont fault along the Lüliang Mountain (Xing et al., 2005). The lower interval of Pliocene Jinzhong group, which represent the oldest Cenozoic deposits in Jinzhong Basin, are mainly consist of conglomerate, sandstone along with other rough clasts, and the upper interval changed to lacustrine mudstone and other fine clastic rock. The rapid subsidence of the graben basins and the intensive uplifting along the mountain rim occurred simultaneously, synchronous growth and decline, thus indicating a rapid uplifting process in the Pliocene of Lüliang Mountain. In the late Miocene (about 10-8Ma), Lüliang Mountain piedmont (east and west sides) accumulated an alluvial fan deposits, Known as Luzigou Formation, mainly composed of conglomerate, which suggests a strong uplifting activities during this period in Luliang Mountain area (Li et al., 2013).

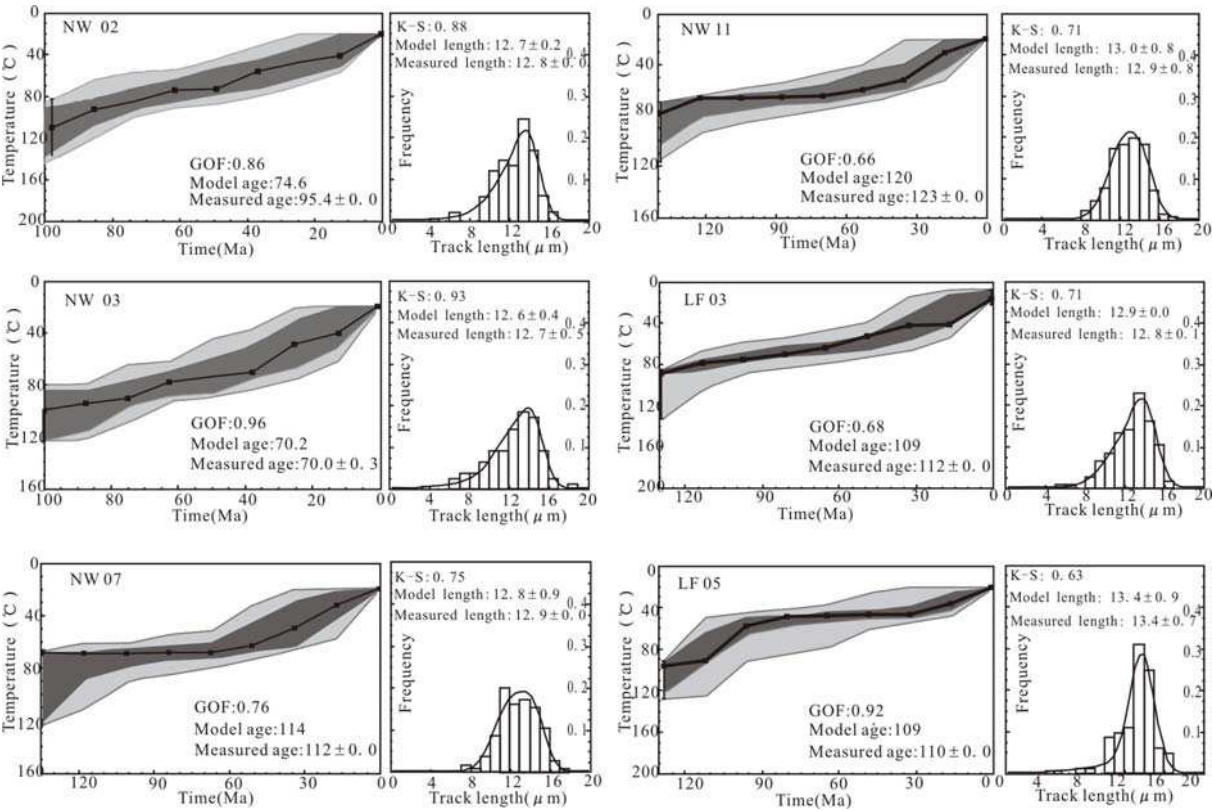


Figure 6 Modeling sketch of time-temperature paths from the Lüliang Mountain

Combined the thermal history modeling of the AFT samples, analysis of the statistic data of the fission track ages data and regional geological evolution history, the uplifting process

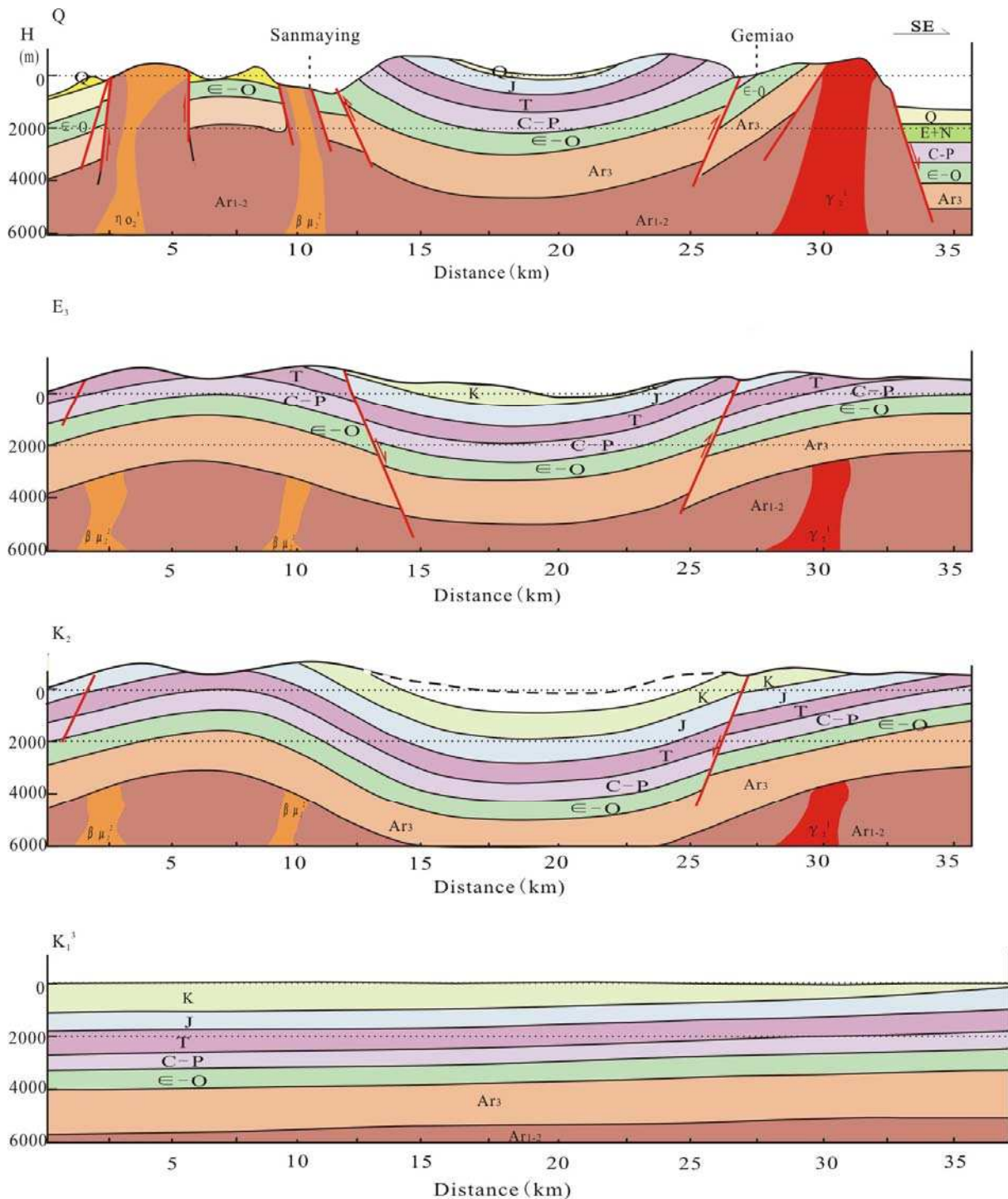


Figure 7 Models illustrating the uplifting and evolution processes of the Lüliang Mountain (taken the north sampling section as an example)

of Lüliang Mountain could be divided into three stages synthetically. (Fig.7) The first stage is slow uplifting (about 120Ma~65Ma), in this period, the studied area was forced by regional compressive stress, and led to folded deformation involved the basement strata. The strata in the core of compound anticline occurred relatively strong uplift and erosion, made the Precambrian basement lifted from the bottom of the annealing zone to the top as a result, but the uplifting of the core of synclines was not obvious. The second stage is the accelerating uplifting (about 65Ma ~23Ma), during this period the uplift process strengthened obviously

and had regional integrity. There was a unified regional dynamic background among the Lüliang Mountain, Ordos Basin and neighboring areas. The last stage is intensive uplifting (about 23Ma to date), which led to the basement rocks of the core of the compound anticline begin to exhumate and uplift to 2000 meters altitude, as well as the Jurassic strata in the core of Ningwu-Jingle syncline uplifted to 2000 meters altitude and suffered denudation (Fig. 7). Uplifting process was further intensified in Pleistocene, which led to the accumulation of gravels along piedmont, which also had the genetic coupling relationship with the eastern neighboring Shanxi Cenozoic graben system.

6 CONCLUSIONS

(1) Fission track analysis based on middle and northern sampling sections suggests that the uplifting activity of the Lüliang Mountain mainly occurred after late Early Cretaceous. Three evolution stages namely slowly uplifting (120Ma- 65Ma), accelerated uplifting (65Ma- 23Ma), and intensive uplifting (23Ma to date) can be identified, among which the uplifting activity since Cenozoic is the major lifting period. Taken the Lüliang Mountain area as a whole, the lifting activity exhibits non-equilibrium in temporal and spatial aspects. The middle and northern parts of Lüliang Mountain area uplifted after late Early Cretaceous, earlier than the southern part, which is mainly lifted since Miocene. The conclusion based on fission track analysis is consistent with the strata record in the Lüliang Mountain area and neighboring Cenozoic faulted basins.

(2) From Middle Triassic to Early Cretaceous, the Lüliang Mountain area is a part of the large scale Ordos basin. They experienced synchronous subsidence- uplifting processes together. Their evolution differentiation happened since late Early Cretaceous. The intensive uplifting activity especially since Miocene had the genetic coupling relationship with the eastern neighboring Shanxi Cenozoic graben system. Generally, the uplifting and evolution processes of the Lüliang Mountain area since late Early Cretaceous share an unified regional geodynamic setting, accompanied with lifting and dying out of the Mesozoic Ordos basin and development of neighboring Cenozoic faulted grabens, are mainly related to the far field effects of both compression sourced from southwestern Tibet plateau and westward subduction of the Pacific block in Cenozoic.

Acknowledgements

This study was supported by National Natural Science Foundation of China (Grant No. 41330315 and 41002071) and Opening Foundation of State Key Laboratory of Continental Dynamics, Northwest University (Grant No. BJ091354). We would like to thank the reviewers and editors for their helpful suggestions.

References

1. Ye, L. J., 1983. Sedimentary Formation of the North China Platform. Science Press, Beijing. 1-10. (in Chinese)
2. Zhang, K., 1983. The Evolution Properties of a Large Scale Mesozoic Sedimentary Basin in North China Fault-Block Region. *Oil and Gas geology*, 4(2): 202-208. (in Chinese)
3. Li, S. T., Cheng, S. T., Yang, S. G., et al, 1992. Sequence Stratigraphy and Depositional System Analysis of the Northeastern Ordos Basin. *Geological Publishing House*, Beijing. 1-12. (in Chinese)

4. Sun, G. F., Li, J. P., Liu, K. Q., et al, 1985. Evolution of a Major Mesozoic Continental Basin within North China Plate and Its Geodynamic Setting. *Oil and Gas Geology*, 6(3): 280-286.(in Chinese with English Abstract)
5. Liu, C. Y., Zhao, H. G., Zhao, J. F., et al, 2008. Temporal- spatial Coordinates of Evolution of the Ordos Basin and its Mineralization Responses. *Acta Geologica Sinica (English Edition)*, 82(6): 1229-1243.
6. Cheng, S. T., Huang, Y. Q., Fu, X. H., 1997. Paleogeography Reconstruction of the Early- Middle Jurassic Large Ordos Basin and Development and Evolution of Continental Down-Warping. *Acta Sedimentologica Sinica*, (15): 43-49. (in Chinese with English Abstract)
7. Wang S. M., Zhang, Y. P., 1999. Study on the Formation, Evolution and Coal-accumulating Regularity of the Jurassic Ordos Basin. *Earth Science Frontiers*, 6(App.): 147-155. (in Chinese with English Abstract)
8. Zhang, H., Jin, X. L., Li, G. H., et al, 2008.Original Features and Palaeogeography Evolution During the Jurassic-Cretaceous in the Ordos Basin. *Journal of Palaeogeography*, 10(1):1-11. (in Chinese with English Abstract)
9. Zhao, W. Z., Wang, X. M., Guo, Y. R., et al, 2006. Restoration and Tectonic Reworking of the Late Triassic Basin in Western Ordos Basin. *Petroleum Exploration and Development*, 33(1):6-13. (in Chinese with English Abstract)
10. Yang, M. H., Liu, C. Y., Zeng, P., et al, 2012. Prototypes of Late Triassic Sedimentary Basins of North China Craton (NCC) and Deformation Pattern of its Early Destruction. *Geological Review*, 58(1):1-18. (in Chinese with English Abstract)
11. Shen Q. H., Lu, Z. B., Bai, Y. B., 1963. Some absolute age data rocks dating in the Lüliang- Wutai area. *Geological Review*, 21(3): 154-160. (in Chinese with English Abstract)
12. Geng, Y. S., Wan, Y. S., Shen, Q.H., et al, 2000. Chronological Framework of the Early Precambrian Important Events in the Lüliang Area, Shanxi Province. *Acta Geologica Sinica*, 74(3):216-223. (in Chinese with English Abstract)
13. Xu, C. L., Zhu, G. X., Tan, Y. L., et al, 2008. A Review on Geographic Divisions for Precambrian in the Lüliang Mountains Area. *Geological Review*, 54 (4): 459-465. (in Chinese with English Abstract)
14. Zhao, Z.Y., 1990. Meso-cenozoic Tectonics of the Shanxi Block and its Formation and Evolution. Seeing: Zhao, Z. Y., Liu, C. Y. and Yao, Y. Eds. *The Formation and Evolution of the Sedimentary Basins and Their Hydrocarbon Occurrence in the North China Craton*. Northwestern Polytechnical University Press, Xi An. 75-84. (in Chinese with English Abstract)
15. Timothy, M. K. and Li, J. H., 2003. Paleoproterozoic Tectonic Evolution of the North China Craton. *Journal of Asian Earth Sciences*, 22:383-397.
16. Zhao, G. C., Wilde, S. A., Sun, M., et al., 2008. SHRIMP U-Pb Zircon Ages of Granitoid Rocks in the Lüliang Complex: Implications for the Accretion and Evolution of the Trans-North China Orogen. *Precambrian Research*, 160: 213-226.
17. Zhao, J. F., Liu, C. Y., Wang, X. M., et al., 2009. Uplifting and Evolution Characteristics of the Lüliang Mountain and Its Adjacent Area during Meso - Cenozoic. *Geological Review*, 55 (5): 673-682. (in Chinese with English Abstract)
18. Li, J. X., Yue, L.P., Xu, Y., et al., 2009. Uplift of Lüliang Mountains and Evolution of the Yellow River- Evidence from Gravel Beds in Piedmont. *Scientia Geographica Sinica*, 29(4): 582-586. (in Chinese with English Abstract)
19. Li, J. X., Yue, L. P., Liu, C. Y., et al., 2013. The Tectonic-Sedimentary Evolution of the Lüliang

- Mountain since the Miocene. *Journal of Stratigraphy*, 37(1): 93-100. (in Chinese with English Abstract)
20. Peter W. R., 2005. Past, Present and Future of Thermochronology. *Reviews in Mineralogy and Geochemistry*, 58:1-18.
 21. Donelick R. A., O'Sullivan, P. B., Ketcham, R. A., 2005. Apatite Fission Track Analysis. *Reviews in Mineralogy and Geochemistry*, 58: 49-94.
 22. Liu, S. F., Zhang, G. W., 2005. Fundamental Ideas, Contents and Methods in Study of Basin and Mountain Relationships. *Earth Science Frontiers*, 12(3): 101-111. (in Chinese with English Abstract)
 23. Wang, Q. C. and Li, Z., 2003. Basin-Orogen Coupling and Origin of Sedimentary Basins. *Acta Sedimentologica Sinica*, 21(1):24-30. (in Chinese with English Abstract)
 24. Zhang, G. W., Guo, A. L., Yao A. P., 2006. Basic Research Thinking of China Continental Geology and Continental Tectonic. *Progress in Natural Science*, 16(10): 1210-1215. (in Chinese with English Abstract)
 25. Liu, C. Y., Zhang, D. D., 2009. Characteristics, Thought of Study and Methodology of Complex System of Basin. *Journal of Northwest University (Natural Science Edition)*, 39(3): 350-358. (in Chinese with English Abstract)
 26. Wang, T. H., 1995. Evolutionary Characteristics of Geological Structure and Oil-gas Accumulation in Shanxi-Shaanxi Areas. *Journal of Geological & Mineral Resources in North China*, 10(3):283-398. (in Chinese with English Abstract)
 27. Feng, Z. Z., 1990. Lithofacies Palaeogeography of Early Palaeozoic Era in North China Platform. Geological Publishing House, Beijing. 1-270. (in Chinese)
 28. Shang, G. X., 1997. Coal Geology of the North China Platform in Late Paleozoic. Shanxi Science and Technology Publishing House, Taiyuan. 25-80. (in Chinese)
 29. Fu, S. T., Tian, J. C., Chen, H. D., et al., 2003. The Delta Depositional System Distribution of Late Paleozoic Era in Ordos Basin. *Journal of Chengdu University of Technology (Science & Technology Edition)*, 30(3):236-241. (in Chinese with English Abstract)
 30. Zhao J. F., Liu, C. Y., Wang, X. M., et al., 2010. Reconstruction of the Original Sedimentary Boundary of the Middle Jurassic Zhiluo Formation-Anding Formation in the Ordos Basin. *Acta Geologica Sinica*, 84(2): 553-569. (in Chinese with English Abstract)
 31. Weng, W. F., Liu, C. Y., Zhao, H. G., et al., 2009. Denudation Thickness Restoration of Early Cretaceous Strata in the Ordos Basin. *Journal of Stratigraphy*, 33(4): 373-380. (in Chinese with English Abstract)
 32. Gleadow, A. J. W, Duddy, I. R., Green, P. F., et al., 1986. Confined Fission Track Lengths in Apatite: A Diagnostic Tool for Thermal History Analysis. *Contrib Mineral Petrol*, 94: 405-415.
 33. Green, P. F., 1986. On the Thermo-tectonic Evolution of Northern England: Evidence from Fission Track Analysis. *Geology*, 5: 493-506.
 34. Hurford, A. J., Green, P. F., 1982. A Users' Guides to Fission-track Dating Calibration. *Earth and Planetary Science Letters*, (59) : 343-354.
 35. Liu W. S., Qin, M. K., Qi, F.C., et al., 2008. Analysis on the Meso-Neozoic Subsidence and Uplift History of the Periphery of the Ordos Basin Using Apatite Fission Track. *Uranium Geology*, 24(4): 221-227. (in Chinese with English Abstract)
 36. Liu, C. Y., Zhao, H. G., Zhang C., et al., 2009. The Important Turning Period of Evolution in the Tibet-Himalayan Tectonic Domain. *Earth Science Frontiers*, 16(4): 1-12. (in Chinese with English Abstract)
 37. Ren, Z. L., Zhang, S., Gao, S. L., et al., 2006. Research on Regional Maturation Anomaly and

- Formation Time in the Ordos Basin. *Acta Geologica Sinica*, 80(5):674-684. (in Chinese with English Abstract)
38. Sun, S. H., Li, X. M., Gong, G. L., et al., 1997. The Study of the Tectonic Thermal Event of the Ordos Basin. *Chinese Science Bulletin*, 42(3):306-308.
 39. Yuan, W. M., Yang Z. Q., Zhang, Z. C., et al., 2011. Uplift and denudation of the Huangshan Mountain in Anhui Province. *Science China: Journal of Earth Science*, 41(10): 1435- 1443.
 40. Ketcham, R. A., 2005. Forward and Inverse Modeling of Low-temperature Thermochronometry Data. *Reviews in Mineralogy & Geochemistry*, (58): 275-314.
 41. Xing, Z. Y., Zhao, B., Tu, M. Y. et al., 2005. The Formation of the Fenwei Rift Valley. *Earth Science Frontiers*, 12(2):247-262. (in Chinese with English Abstract)